

Feature Extraction in Digital Fundus Imagery for Diabetic Retinopathy Detection

Teal Hobson-Lowther

*Dept. of Electrical Engineering and Computer Science
Colorado School of Mines
Golden, Colorado
tealhobsonlowther@gmail.com*

May 4, 2015

1 Introduction

Diabetic Retinopathy is a complication of Diabetes that causes eye damage and loss of vision. It occurs when fluctuating glucose levels harm blood vessels in the eye. Initially, these blood vessels rupture and start leaking into the eye, causing it to change shape. The retina bends, and vision becomes skewed. Eventually, in severely developed cases, the eye grows new, weak blood vessels which obscure central vision. If left untreated, this disease can lead to a complete loss of vision.

Early detection of Diabetic Retinopathy (DR) is crucial to effective treatment. Image processing can contribute to this field immensely through the effective application of feature extraction and classification algorithms. The diagnosis of DR by a human requires highly specialized medical training. In areas where there is a lack of specialists, optical images must be sent away to have diagnosis performed. This time delay can lead to loss of communication, and sets treatment back even further [5]. An ideal algorithm for DR detection would therefore be highly precise, relatively inexpensive, and quick. Much work has been done in this field, to be discussed in Section 2.

There are four levels of Diabetic Retinopathy, and they are divided into two classes [1], and shown in Figure 1:

1. Non-Proliferate Diabetic Retinopathy (NPDR):

- *Mild NPDR (1):*

The eye has at least one micro-aneurysm, may or may not have hemorrhages, cotton wool spots, or exudates. [Figure 1a]

- *Moderate NPDR (2):*

Many micro-aneurysms and hemorrhages. Limited amount of venous beading can be seen, as well as cotton-wool spots. [Figure 1b]

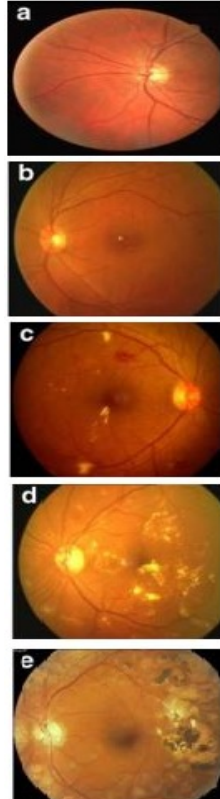


Figure 1: Progressive stages of DR Development: a) No signs of DR b) Mild NPDR c) Moderate NPDR d) Severe NPDR e) PDR [1]

- *Severe NPDR (3):*

The **(4 – 2 – 1)** rule classifies the last case of NPDR [Figure 1c].

This classification is achieved if any of the following are met:

- (a) Numerous hemorrhages or micro-aneurysms in **4** quadrants of the eye
- (b) Venous beading in **2** or more quadrants
- (c) Intra-retinal abnormalities in at least **1** quadrant.

2. *Proliferate Diabetic Retinopathy (PDR) (4):* New, fragile blood vessels

are generated by the eye in response to the massive damage done in the previous stages.

These new blood vessels are highly susceptible to leaking, and cloud the vitreous gel with blood, causing severe vision loss and even blindness. [Figure 1e]

Although image-processing and algorithms for classification are generally paired in papers on this topic, no effort will be given to actually automate the classification of different levels of DR in digital fundus imagery. Focus will be solely on the image-processing techniques generally used in the feature-extraction which could be used later for classification systems.

This paper is formatted as follows: Section 2 is devoted to a short (and by no means exhaustive) description of previous work in the application of image processing techniques to the area of Diabetic Retinopathy. Section 3 describes the data to be analyzed, and several properties that make it difficult to work with. Section 4 shows the methodology behind the feature extraction that will be implemented. Specifically, Section 4.1 is dedicated to the methodology behind pre-processing the data, Section 4.2 gives an outline of the algorithm for blood-vessel detection and extraction, and Section 4.3 gives a treatment of the process for exudate detection. Section 5 describes the application of these algorithms to multiple images, and the performance is quantified. Section 6 summarizes and discusses the results of these experiments, and points out any especially interesting features held therein. Section 7 delineates future work to be performed, based on the successes/failures found in the previous sections.

2 Previous Work

Due to the large number of people effected by this disease, it is a well researched and documented subject. There have been several groups of scientists who have approached the issue of computational diagnosis of Diabetic Retinopathy over the past 20 years. The approaches taken to accomplish feature extraction and image classification are highly diverse, and there has been notable progress made toward this goal.

A wonderful review of the most well-known approaches is given in [1]. This not only provides a thorough and concise summary of the work done, but also a wealth of references to papers on the matter. It also contains a useful table summarizing different approaches and their effectiveness, seen in Table 1. Some methods simply classify based on a binary system, either the eye is healthy or it has Diabetic Retinopathy of some stage of development. Others use a three, four, or five class system depending on the level of detail desired by the researchers. AdaBoost classification algorithms are applied to extract blood vessels in [2]. Ridge-based segmentation classification techniques to detect blood vessels are used in [3]. Trace transform feature detection approaches and Support-Vector Machine classification methods are investigated in [4].

Detailed, extensive descriptions of image-processing techniques for feature extraction are given in [5], and the processes described therein will serve as the ground-layer for my algorithms. One especially useful feature of this source is the flow-chart style pseudo-code that accompanies the

Table 1 Comparison of different classification methods

Authors	No of classes	Method	Accuracy of classification	Sensitivity	Specificity
Wang et al. 2000 [73]	2	Minimum distance discriminant classifier	70%		
Sinthanayothin et al. 2003 [66]	2	Moat operator	Not reported	80%	71%
Usher et al. 2003 [82]	2	Lesions	Not reported	95%	53%
Singalavanija et al. 2005 [81]	2	Blood vessels, exudates, haemorrhages, microaneurysms	Not reported	75%	83%
Lee et al. 2005 [43]	3	Hemorrhages, microaneurysms, hard exudates, cotton wool spots	Max: 88%	Not reported	Not reported
Neubauer et al. 2005 [50]	2	Retinal thickness analyzer	Not reported	93%	100%
Kahai et al. 2006 [36]	2	Decision support system (DSS)	Not reported	100%	63%
Philip et al. 2007 [57]	2	Exudates	Not reported	91%	67%
Estabridis and Figueiredo 2007 [20]	2	Fovea, blood vessel network, optic disk, bright and dark lesions	90%	Not reported	Not reported
Li et al. 2008 [46]	2	Bright lesions, retinal vessel patterns	Not reported	81%	Not reported
Abràmoff et al. 2008 [2]	3	Optic disc, retinal vessels, hemorrhages, microaneurysms, vascular, abnormalities, exudates, cotton wool spots, drusen	Not reported	84%	64%
Wong et al. 2008 [75]	4	Area of blood vessel	84%	92%	100%
Nayak et al. 2008 [48]	3	Blood vessels, exudates and texture	94%	90%	100%
Acharya et al. 2008 [3]	5	Higher order spectra	82%	83%	89%
Acharya et al. 2009 [5]	5	Blood vessel, exudates, microaneurysms, haemorrhages	86%	82%	86%
Vujosevic et al. 2009 [71]	2	Single lesions	Not reported	82%	92%

Table 1: Short Summary of Previous Work in DR Detection

descriptions. I was able to use the techniques learned from class to execute the several relatively intricate steps to achieve quite successful results.

3 Data

The data that was used in the algorithms below were provided by Kaggle [5]. It consists of over 30,000 digital fundus photographs taken from a variety of cameras, in a variety of conditions. There is a large amount of noise in the imagery, as is generally the case with these images. The images are very high-resolution, with a wide range of size, lighting conditions, noise levels, eye orientation, and framing. The data-set has an associated .csv file containing ranks of each image, hand-labeled by human specialists from 0-4 (described in Section 1). A sample of several digital fundus images, with different photographic conditions, is shown in Figure 2.



Figure 2: Examples of digital fundus imagery, taken from different cameras, with varying levels of DR. Notice the widely varying noise and illumination conditions that make pre-processing essential for feature extraction.



Figure 3: Digital Fundus images after several stages of pre-processing, as described in Section 4.1. a) Image has green channel extracted and has been normalized. b) Image has had intensities inverted. c) Edges have been detected.

4 Methods

The methodology used in this paper is separated into four parts, pertaining to the four stages of feature detection. Section 4.1 delineates the pre-processing algorithms used on the images. Section 4.2 describes the process for blood-vessel detection. Section 4.3 explains exudate detection.

4.1 Pre-Processing

As mentioned before, the methodology for pre-processing is borrowed from [5]. The algorithm for this process can be found in Appendix A. The results of each step of this process are presented in Figure 3.

4.1.1 Taking the Green Channel

To begin the image pre-processing, we first take the RGB image and select only the green channel. Hemoglobin in the blood stream absorbs green light, and so observing the blood vessels will be most successful on this channel. This technique was borrowed from several papers on the topic; [1], [2]. [3], [4], and [5] use this approach.

4.1.2 Normalizing Image

Once the green channel has been selected, we must convert the image to gray-scale and normalize the image. This turns the image into a matrix of intensity values ranging from 0-1.

4.1.3 Image Inversion

After image normalization, an inverted version of the image must be created for certain parts of the feature-extraction process. This transforms all intensity values obtained from the normalization operation to their complement. If the intensity was of a single pixel after normalization α , the new pixel value is $1 - \alpha$, for each pixel in the image.

4.1.4 Edge-Detection

For most of the feature detection algorithms, it is helpful to extract the edge of an image before filling it. Therefore, the following steps for edge-detection were executed during the pre-processing stage as well:

1. Perform image inversion as described in 4.1.1 - 4.1.3.
2. Erode and dilate the image using a disc-sized structuring element of size 8. This has the effect of blurring everything which does not have a consistently smooth curvature, and highlighting edges.
3. Subtract the eroded image from the dilated one. This eliminates all but the edge from the image.
4. Binarize the image, leaving it black and white.

4.2 Blood-Vessel Detection

Blood vessels look like branching networks of lines in the eye. Isolating the blood vessels consists of removing portions of the fundus image that do not have long, continuous shapes. This amounts to subtracting images that are opened using disk shaped structuring elements from the original. The algorithm for this process can be found in Appendix C. Once again, we borrow methods from [5].

The several stages of image processing described in this section are summarized in Figures 4 and 5. The results of applying the algorithm both to a healthy eye and to an eye with Mild NPDR are shown in 4 and 5, respectively.

4.2.1 Adaptive Histogram Equalization

Adaptive histogram equalization (AHE) is a way to distribute illumination across an image, as well as to increase contrast. This operation is performed so we may increase contrast on edges of blood vessels [Figures 4,5 (a)].

4.2.2 Morphological Opening

After AHE, morphological opening is performed to reveal any roundly-shaped artifacts of the image. For this opening, we use a disk-shaped structuring element of size 8 [Figures 4,5 (b)].

4.2.3 Image Subtraction

Now the resultant image from Section 4.2.2 is subtracted from the result of Section 4.2.1. The resultant image is one in which only the shapes with long edges and points remain. This isolates the blood-vessels and makes them stand out [Figures 4,5 (c)].

Figure 4: The results of several stages of processing for blood vessel feature extraction on a healthy eye: a) Adaptive histogram equalization as been applied. b) Morphological opening with disk-shaped element. c) Subtraction of opened image from high-contrast AHE image. d) Binarize the image. e) Median filter and subtraction of edge from resultant image. f) Fill holes after removing boundary. While there are some artifacts due to noise, the extension of the blood-vessel network is quite clear.

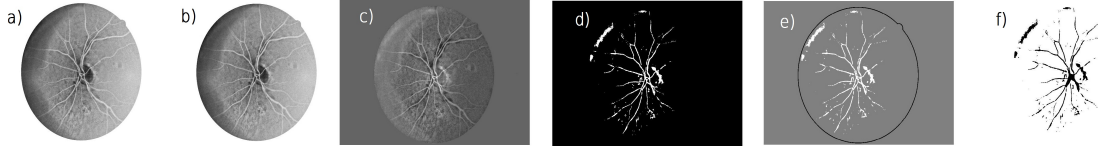
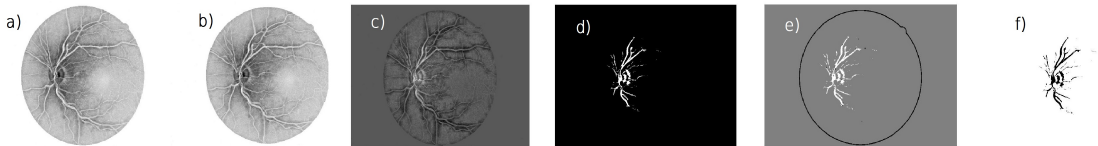


Figure 5: The results of several stages of processing for blood vessel feature extraction on an eye with Mild NPDR. Images are at same stages in process as in Figure 3. The extension of the blood-vessel network compared to Figure 3 is small, indicating damage to blood vessels due to DR.



4.2.4 Binarize Image

We apply a threshold found experimentally to binarize the result of Section 4.2.3. The resulting image contains the blood vessels in white and the rest of the eye in black [Figures 4,5 (d)].

4.2.5 Median Filter Image

A median filter is applied to the image, smoothing out the image.

4.2.6 Subtract Boundary Image

The boundary image from Section 4.1.4 is subtracted from the median filtered image [Figures 4,5 (e)].

4.2.7 Fill Holes/Remove Boundary

Now the image is ready for an image filling and final inversion, the result of which is an image with the detected blood-vessels in black and a white background, with no edge, around. We may

use this image to calculate the ratio of blood-vessel area to total area of the eye, and use this as a feature to feed a classification algorithm [Figures 4,5 (f)].

4.3 Exudate Detection

Exudates are places where the blood vessels are exuding small spots of liquid into the eye. They look like tiny white spots in the fundus imagery. The general strategy is to use round structuring elements to reveal these shapes, and then isolate them from the rest of the image. The algorithm for exudate detection can be found in Appendix E. The results of the processes in this section are shown in Figures 6 and 7.

Figure 6: The several steps of exudate detection performed on a healthy eye. a) Fundus image after disk opening. b) Image after octagonal opening. c) Result of large octagonal opening. d) Final black and white thresholding. No exudates are detected.

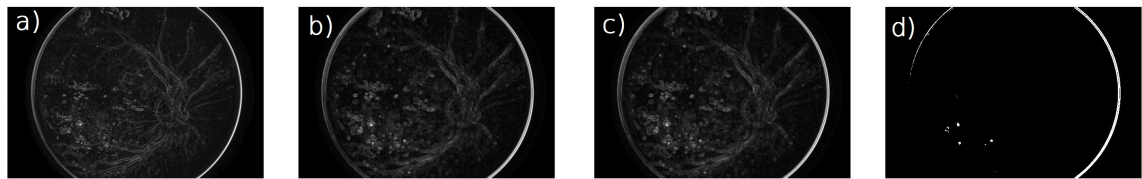
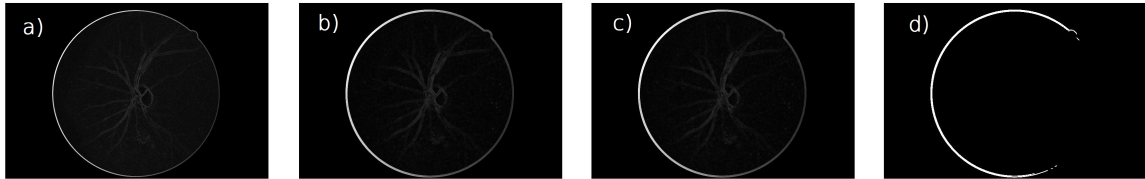


Figure 7: The results of exudate detection on an eye with PDR. The images are taken from the same parts of the process as Figure 6. Three exudates are detected.

4.3.1 Octagon/Disk Morphological Operations

The image is opened with a series of structuring elements to highlight the shape of the exudate. First, a disk-shaped element of size 8 was applied [Figures 6,7 (a)]. An octagonal structuring element of size 9 was then used to open the image again [Figures 6,7 (b)]. A larger octagonal element, of size 30, was used to open the image a third time. [Figures 6,7 (c)]

4.3.2 Binarization and Final Opening

Threshold values of .3, found experimentally, are applied to the results of Section 4.3.1 to give us a black and white image of the exudates. A final disk-shaped structuring element is used to open the image [Figures 6,7 (d)].

5 Experiments/Results

Experiments were performed on a test data set containing 10 sample images. The images were hand-labeled with rankings from 0-4 by a optical pathologist before the data were analyzed.

5.1 Pre-Processing

To determine the effects of pre-processing on the image, we calculate the means and variances of each image after taking the green channel (initial values) and after normalizing the image (final values). The results are summarized in Table 2. The code used to run the preprocessing is described in Appendix A. The code used to find the means and variances of the images is shown in Appendix B

The initial means and variances of the green channel of the image are quite high, but normalization reduces these numbers immensely. This indicates that our image has, indeed, been normalized.

File Name	Green Ch. Mean	Norm. Mean	Green Ch. Variance (E6)	Norm. Variance
10_left	54.572	0.2140	6.2350	0.0015
10_right	24.250	0.1865	0.0666	0.00023
13_left	48.205	0.1890	0.6797	0.0002
13_right	48.866	0.1916	0.9218	0.00022
15_left	54.951	0.2431	1.2167	0.0005
15_right	58.167	0.2394	2.0060	0.00058
16_left	92.236	0.3843	4.2404	0.0013
16_right	82.950	0.3253	0.9448	0.00022
17_left	37.759	0.1504	0.5597	0.0001
17_right	45.405	0.1781	0.7561	0.00018

Table 2: Mean and Variance of Images, Before and After Pre-processing

5.2 Blood-Vessel Detection

To analyze the effects of our blood-vessel extraction algorithm (described in Section 4.2), we will look at the total area of the blood-vessels, normalized in comparison to the total area of the optical image. We will use the DR_BVD function (Appendix C) to perform the detection, and then use the DR_BVD_Analysis script (Appendix D) to determine these values. This will be accomplished by summing the pixels that indicate blood vessels, and normalizing to be consistent across several camera types. The results of this process are summarized in Table 3.

The general idea is that, as blood vessels begin to become damaged due to DR, they will initially reduce in total area, and then increase in the final stage (PDR), as new blood-vessels are formed to replace damaged ones. The results of my experiment show that my algorithm is not very effective in classifying DR based on blood-vessel area. Area that is found as a result of this procedure does not strongly indicate DR development. Additionally, in some cases (such as images 13_left and 13_right), looking at the area alone would cause a mis-classification of 4 (large area), when in fact it is truly classified as a 0 (no DR).

The most likely reason for this is the thresholding level built into the algorithm. We need a thresholding technique that is adaptive, and based on the illumination of the figure in its initial

state. Because we use the same thresholding value for each image, we fail to have an algorithm that is robust to variations in illumination levels. An additional stage of pre-processing, where we adjust the illumination levels of all images to a normalized value, I believe, would help to remedy this situation.

5.3 Exudate Detection

In this experiment, we run the algorithms described in Section 4.3 on the same set of samples described in Section 5.2, and manually count the number of exudates detected. We ignore results that appear to be blood vessels, mis-classified as exudates. If an exudate is detected, the image should be classified as at least rank 1. The results of this experiment, including the resultant images and total number of exudates detected, are shown in Table 4.

As we can see, this algorithm is much more successful in indicating the rank of the fundus image than the blood vessel detection algorithm. All optical images of rank 0 were correctly diagnosed. The most exudates (3,5) were detected in the rank 4 eye, as is to be expected. The lower ranks generally had 2 exudates. Classifying the eye based on exudate number alone would yield a much more precise result than that of the blood-vessel detection algorithm.

6 Conclusions

The results of the blood vessel detection algorithm were spotty, at best. While the performance on some images was satisfactory, issues in uniformity of illumination yielded horrible results on images such as 13_left and 13_right. These issues will need to be addressed if I wish to use this algorithm to correctly classify the rank of development in Diabetic Retinopathy. That being said, in the papers I have read, the networks of blood vessels that were able to be detected were much more extensive. I would want my algorithm to generate images of blood vessels with much higher resolution than those obtained in the preceding experiments, because rank 4 DR requires a visualization and tracking of tiny, newly developed blood-vessels.

The results of my exudate detection algorithm were much more successful. If the methods of hand-counting the exudates that I used could be extended into another algorithm, and the same results could be produced, we would have a workable, convincing ground-level idea of how developed a patient's DR is with the results of this algorithm alone. This is quite exciting. In fact, although the sample size was quite small, we actually had 100% classification of rank 0 DR due to the number of exudates detected by this algorithm and counting-process being 0.

Although these two feature-extraction methods are a good starting point for the project, I have found that the correct diagnosis of DR is a very complex and intricate issue. There are several factors to be considered, and blood vessel extension and exudate counts alone would not be extremely effective for diagnosis. That being said, I believe that the incorporation of other features into a classification algorithm could be quite successful based on the initial investigations conducted in this paper.

7 Future Work

This project has generated much future work. For starters, I would like to develop algorithms which can detect other features shown to be useful to DR detection, such as micro-aneurysm and hemorrhage detection, as well as texture analysis. These features would probably be extremely helpful in the diagnosis of DR.

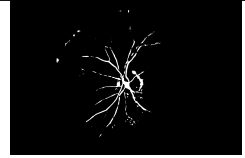
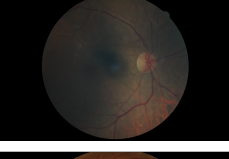
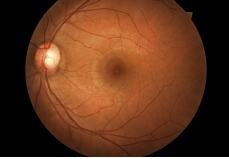
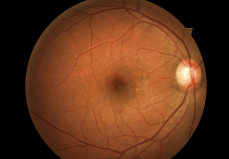
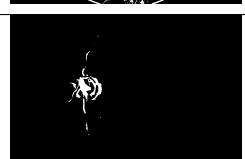
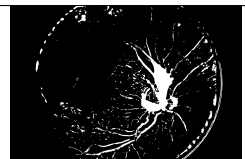
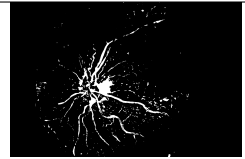
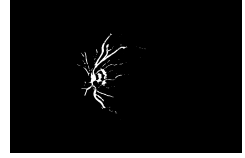
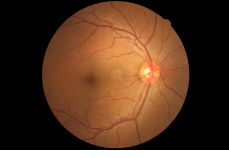
Image Name	Original Image	Blood-Vessel Image	Blood Vessel Area (px,E7)	Rank (0-4)
10_left			6.17	0
10_right			1.98	0
13_left			65.7	0
13_right			66.6	0
15_left			4.3	1
15_right			4.69	2
16_left			17.1	4
16_right			9.36	4
17_left			3.00	0
17_right			5.37	1

Table 3: Effects and Comparative Area of Blood-Vessel Detection Algorithm
10

Image Name	Original Image	Exudate Image	Number of Exudates	Rank (0-4)
10_left			0	0
10_right			0	0
13_left			0	0
13_right			0	0
15_left			2	1
15_right			2	2
16_left			3	4
16_right			5	4
17_left			0	0
17_right			2	1

Table 4: Results of Exudate Detection on 10 Images, with Number of Detected Exudates and True Rank

Additionally, I would like to make some alterations to the pre-processing stage, to try to make more uniform normalized illumination levels. After this is implemented, perhaps a more flexible binary thresholding method, such as Otsu's, could be utilized to generate more accurate and consistent images of the blood vessel networks.

Future work in exudate detection would involve incorporating an algorithm to count exudates in the manner employed in Section 5.3. This would probably involve selecting areas with region properties similar to those I looked for, namely those that are more circular in nature.

The largest, and most important piece of future work involved in accurate DR diagnosis is the implementation of a classification algorithm. Several machine learning algorithms would be effective for this process, but these are only as effective as the feature-extraction methods used before classification. I would like to see a neural-network applied to this situation, to see if it can discover methods of classification, the complexity of which would be unobtainable by human eyes.

References

- [1] Faust, Oliver, Rajendra Acharya U., E. Y. K. Ng, Kwan-Hoong Ng, and Jasjit S. Suri. "Algorithms for the Automated Detection of Diabetic Retinopathy Using Digital Fundus Images: A Review." *Journal of Medical Systems* 36.1 (2012): 145-57. Web.
- [2] Lupascu, Carmen A., Domenico Tegolo, and Emanuele Trucco. "FABC: Retinal Vessel Segmentation Using AdaBoost." *IEEE Transactions on Information Technology in Biomedicine* 14.5 (2010): 1267-274. Print.
- [3] Staal, J., M.d. Abramoff, M. Niemeijer, M.a. Viergever, and B. Van Ginneken. "Ridge-Based Vessel Segmentation in Color Images of the Retina." *IEEE Transactions on Medical Imaging* 23.4 (2004): 501-09. Web.
- [4] K. Ganesan, R. Martis, U. Acharya, C. Chua, L. Min, E. Ng and A. Laude, 'Computer-aided diabetic retinopathy detection using trace transforms on digital fundus images', *Medical & Biological Engineering & Computing*, vol. 52, no. 8, pp. 663-672, 2014.
- [5] S. Dua, R. Acharya U and Y. Ng, Computational analysis of the human eye with applications. Singapore: World Scientific, 2011.
- [6] Kaggle.com, 'Kaggle: The Home of Data Science', 2015. [Online]. Available: <http://kaggle.com/c/diabetic-retinopathy-detection>. [Accessed: 02- May- 2015].

Appendices

This appendix contains the code used to perform the feature extraction in the paper above. Code was implemented using Matlab and by following the techniques outlined in [5]. The code is original and developed by the author, with guidance from [5].

A Pre-Processing

```
%%
%Diabetic Retinopathy Preprocessing:
%This function takes a grayscale image of an eye and runs
%algorithms to preprocess the data.
function [Green,Normal,Inverted,Edge] = DR_Pre(IL)
%Input IL is the green channel of an image of an eye.
%Output Green is a green-channel version of the input, IL.
%Output Normal is the Normalized version of Green.
%Output Inverted is the Inverted Version of Normal.
%Output Edge is the edge-detected version of IL.

%Verify the image is green channel:
if size(IL,3) > 1
    IL = IL(:,:,2);
end
Green = IL;
%%
%Convert to grayscale:
IL = mat2gray(IL);
Normal = IL;
%%
%Invert image in intensity:
IL = imadjust(IL,[0;1],[1;0]);
Inverted = IL;
%%
%Detect Boundary of Image:
IL1 = edge(IL,'sobel',.05);
%%
>Create Disc Structuring Element, size 8:
SD = strel('disk',8);
%%
%T1 = Eroded image:
T1 = imerode(IL1,SD);
%%
%T2 = Dilated image:
T2 = imdilate(IL1,SD);
%%
D = T2-T1;
%%
```

```

%Binarised image D --> B1:
B1 = im2bw(D,.099);
%%
Edge = B1;

%%
%Plot the different stages:
figure();
subplot(1,4,1);
imshow(Green,[]);
subplot(1,4,2);
imshow(Normal,[]);
subplot(1,4,3);
imshow(Inverted,[]);
subplot(1,4,4);
imshow(Edge,[]);
end

```

B Pre-Processing Analysis

```

clear all; close all;
k = 20;
l=1;
Meanl = zeros(2,5);
Meanr = zeros(2,5);
Varl = zeros(2,5);
Varr = zeros(2,5);
list = [10, 13, 15, 16, 17];
for i=list
    imstrl = sprintf('%d_left.jpeg',i);
    imstrr = sprintf('%d_right.jpeg',i);
    try
        Left = imread(imstrl);
        Right = imread(imstrr);
        %Perform Pre-Processing:
        [LGreen,LNormal,LInverted,LEdge] = DR_Pre(Left);
        [RGreen,RNormal,RInverted,REdge] = DR_Pre(Right);
        %Calculate mean of images:
        Meanl(:,1) = [mean(mean(LGreen));
                      mean(mean(LNormal))];
        Meanr(:,1) = [mean(mean(RGreen));
                      mean(mean(RNormal))];
        %Calculate variances of images:
        Varl(:,1) = [var(var(double(LGreen)));
                     var(var(double(LNormal)))] ;
        Varr(:,1) = [var(var(double(RGreen)));
                     var(var(double(RNormal)))] ;
    catch

```

```

    end
    l=l+1;
end

C Blood-Vessel Detection

<%
%Blood Vessel Detection for Preliminary Feature Extraction:
%Diaabetic Retinopathy Preprocessing
%This function takes a grayscale image of an eye and runs
%algorithms to enhance and isolate blood vessels. The process
%is described by Acharya, et al.
function [ I ] = DR_BVD( IL )

%Input IL is the green channel of an image of an eye.
%Output I is a binary blood vessel image.

%Verify the image is green channel:
if size(IL,3) > 1
    IL = IL(:,:,2);
end

%Path 1:
%Convert to grayscale:
IL = mat2gray(IL);
%
%Invert image in intensity:
IL = imadjust(IL,[0;1],[1;0]);
%
%Detect Boundary of Image:
IL1 = edge(IL,'sobel',.05);
%
%Create Disc Structuring Element, size 8:
SD = strel('disk',8);
%
%T1 = Erode image:
T1 = imerode(IL1,SD);
%
%T2 = Dilate image:
T2 = imdilate(IL1,SD);
%
%D = T2-T1:
D = T2-T1;
%
%Binarised image D --> B1:
B1 = im2bw(D,.099);
%

```

```

%Path 2:
%Adaptive Histogram Equalization:
ILA = adapthisteq(IL,'NumTiles',[56 56],...
    'NBins',2048,'Distribution','uniform','ClipLimit',.008);

%Create 'ball' structuring element, size 8:
SB = strel('ball',8,8);
%%
%Morphological Opening:
IL2 = imopen(ILA,SB);
%%
%Subtract from Contrasted Image:
IL2 = ILA - IL;
%%
%Binarised Image, B2:
B2 = im2bw(IL2,.099);
%%
%Median Filtered Image, B3:
B3 = medfilt2(B2,[8 8]);
%%
%Paths Meet:
%B3-B1 = Image with Boundary:
B4 = B3-B1;
%%
%Final Image: Imfill to fill holes and remove boundary:
I = imfill(B4,'holes');
I = ~I;
figure(1);
imshow(I,[]);
end

```

D Blood-Vessel Detection Analysis

```

%%
%Diaabetic Retinopathy BVD_Analysis_1:
%Input IL is the green channel of an image of an eye.
%Areal, Arear are vectors containing the ratio of
%blood vessels to total image area.
list = [10, 13, 15, 16, 17];
l=1;
Areal = [];
Arear = [];
for i=list
    imstrl = sprintf('%d_left.jpeg',i);
    imstrr = sprintf('%d_right.jpeg',i);
    try
        Left = imread(imstrl);
        Right = imread(imstrr);
    end
end

```

```

%Perform Pre-Processing:
[LBVD] = DR_BVD( Left );
[RBVD] = DR_BVD( Right );
LBVD = ~LBVD;
RBVD = ~RBVD;
Areal(1) = sum(sum(LBVD));
Arear(1) = sum(sum(RBVD));
imstr12 = strcat('BVD',imstr1);
imstrr2 = strcat('BVD',imstrr);
imwrite(LBVD,imstr12);
imwrite(RBVD,imstrr2);
catch
end
l=l+1;
end

```

E Exudate Detection

```

%%DR_ED This function performs morphological openings and
%image processing techniques to attempt to detect exudates
%for the diagnosis of Diabetic Retinopathy.
%This exuade image can be used as a feature vector for an ANN
%classifier.
function [Img,B1] = DR_ED(IL)

%Grab the green channel of the image only, if not already done:
if size(IL) > 1
    IL = IL(:,:,2);
end
%Convert image to grayscale:
IL = mat2gray(IL);
%Invert the image:
%Dilation and Erosion using octagon and disc-shaped structuring elements:
SO = strel('octagon',9);
SOBig = strel('octagon',27);
SDBig = strel('disk',25);
%Path 1:
%Detect Boundary of Image:
IL1 = edge(IL,'sobel',.05);
%%
%Create Disc Structuring Element, size 8:
SD = strel('disk',10);
%%
%T1 = Erode image:
T1 = imerode(IL1,SD);
%%
%T2 = Dilate image:
T2 = imdilate(IL1,SD);

```

```

%%  

T = T2-T1;  

%%  

%Binarised image D --> B1:  

B1 = im2bw(T,.099);  

B1 = imfill(B1,'holes');  

D1 = imerode(IL,SO);  

D2 = imdilate(IL,SO);  

D = D2-D1;  

Q1 = imerode(D,SD);  

Q2 = imdilate(D,SD);  

Img = Q2-Q1;  

%Closing using octagon shaped structuring element:  

imclose(Img,SOBig);  

%  

% Img = colfilt(Img,[20 20], 'sliding ', @mean);  

% Img = imopen(Img, SBig);  

Img = im2bw(Img,.3);  

figure(666);  

imshow(Img,[]);  

impixelinfo();  

end

```